Renewable Energy xxx (xxxx) 1–14

Contents lists available at ScienceDirect

Renewable Energy

journal homepage: www.elsevier.com/locate/renene

New approach for analysing the effect of minor and major solar cooker design changes: Influence of height trivet on the power of a funnel cooker

Xabier Apaolaza-Pagoaga [a, *], Antonio Carrillo-Andrés [a], Celestino Rodrigues Ruivo [b, c]

[a] Energy Research Group, Department of Mechanical, Thermal and Fluids Engineering, University of Malaga, Calle Arquitecto Francisco Peñalosa, 6, 29071, Malaga, Spain
[b] Department of Mechanical Engineering, Institute of Engineering, University of Algarve, Campus da Penha, 8005-139, Faro, Portugal
[c] ADAI - LAETA, Rua Pedro Hispano nº12, 3030-289, Coimbra, Portugal

ARTICLE INFO

Article history:
Received 22 May 2021
Received in revised form 22 July 2021
Accepted 7 August 2021

Keywords:
Solar cooking
Funnel cooker
Experimental test
Side by side
Trivet

ABSTRACT

In present work, the power values of two funnel cookers were determined by following the standard ASAE S580.1 procedure and also a novel improved approach for better analysing the effect of minor design changes. This new approach is based on experimental side by side tests of the two cookers and it adopts a shorter time interval and a curve fitting based on the LOESS adjustment is adopted for the evaluation of the difference in power values of the different designs tested. The two funnel cookers were tested experimentally with a load ratio of 4 kg m^{-2}. The influence of the height of a trivet, from 0 to 100 mm, on the cooker power was evaluated. The estimated changes in power values due to the design changes were low but not negligible. As example, the power standardised increases 6 W when a height trivet of 25 mm is used respecting cooking operation without trivet. The novel approach is promising because it enables to determine the impact of minor design changes on the power of the cooker. The same analysis is not possible to be performed with the standard ASAE S580.1 procedure due to the uncontrollability of the weather conditions.

Nomenclature

a	Slope of the linear regression of standardised power (W ºC^{-1})
c_w	Specific heat of water (J K^{-1} kg^{-1})
h_T	Trivet height (mm)
I	Solar irradiance (W m^{-2})
I_{bn}	Beam normal solar irradiance (W m^{-2})
$\bar{I}_{bn}$	Average beam normal solar irradiance during a test (W m^{-2})
I_n	Global normal solar irradiance, i.e., global solar irradiance on the plane normal to beam radiation (W m^{-2})
$\bar{I}_n$	Average global normal solar irradiance during a test (W m^{-2})
m_w	Mass of water (kg)
n_p	Number of valid observation points for deriving the linear regression
n_t	Number of tests
n_{t1}	Number of tests performed with cooker CSR1
n_{t2}	Number of tests performed with cooker CSR2
$\dot{Q}$	Cooker power (W)
$\dot{Q}_S$	Standardised cooker power (W)
$\dot{Q}_{S,0}$	Standardised cooker power for $\Delta T_{w,a} = 0ºC$ (W)
$\dot{Q}_{S,50}$	Standardised cooker power for $\Delta T_{w,a} = 50ºC$ (W)
$\dot{Q}_{S,CI95\%}95$	% confidence interval for the standardised power (W)
$\dot{Q}_{S,PI95\%}95$	% prediction interval for the standardised power (W)
$\dot{Q}_{S,Ti}$	Standardised cooker power for trivet *Ti* (T0; T25; T50 and T100) (W)
$\dot{Q}_{S,Tj}$	Standardised cooker power for trivet *Tj* (T0; T25; T50 and T100) (W)
R^2	Coefficient of determination (-)
T_a	Ambient temperature (ºC)
$\bar{T}_a$	Average ambient temperature during a test (ºC)
$\bar{T}_w$	Average water temperature during a test (ºC)
v_a	Wind velocity (m s^{-1})
$\bar{v}_a$	Average wind velocity during a test (m s^{-1})

* Corresponding author.
E-mail address: apaolaza@uma.es (X. Apaolaza-Pagoaga).

https://doi.org/10.1016/j.renene.2021.08.025
0960-1481/

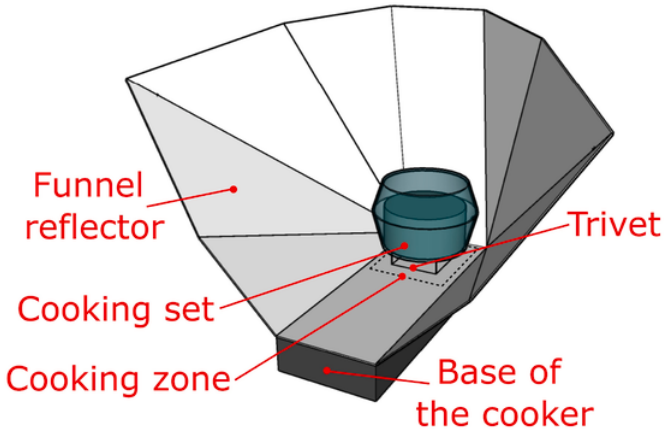

Fig. 1. Schema of the funnel cooker with the main components.

Greek symbols

α_s	Solar altitude angle (º).
$\bar{\alpha}_s$	Average solar altitude angle during a test (º).
$\Delta\dot{Q}_S$	Residual standardized power (W)
Δt_i	Time interval (s)
$\Delta T_{w,i}$	The water temperature increases for each time interval (ºC)
$\Delta T_{w,a}$	Difference between water load and air temperature (ºC)

Subscripts

n	Direction normal to beam radiation
i	Time interval *i*

Abbreviations

CSR1	Solar funnel cooker number 1
CSR2	Solar funnel cooker number 2
LOESS	Locally estimated scatterplot smoothing
SSCAL	Experiment with two cookers tested side by side and using the same trivet height or without using any trivet

1. Introduction

Many solar cooker designs have been developed around the world, with different technologies, different materials [1–4] and new designs [5–7]. Most of long life powerful solar cookers are manufactured with expensive materials [8–10]. Solar cooking systems with storage of sensible or latent thermal energy allow cooking in a wider range of weather conditions, but only few are used in practice [11]. On the opposite side, most panel type solar cookers are low cost devices and construction process is ease. They are composed of different reflective panels that concentrate the sun's radiation in the cooking zone, where the cooking set is placed. The power of this devices is relatively low. So, a transparent enclosure acting as a greenhouse reduces thermal losses of the cooking set is usually required. Many of these designs and their performance data, obtained by using the ASAE S580.1 [12] standard, are available [4].

The ASAE S580.1 standard allows the characterization of a solar cooker performance under standardized conditions in terms of a reference value of standardised power, which can be used to compare the performance between different design of cookers. The use of the standard procedure also enables of the analysis of design changes that are made in a particular cooker when those changes produce important variation of the standardised power. As an example, the standard procedure was adopted by Ruivo et al. [13] to investigate the influence of using a glass or a metal lid on the power of a funnel cooker operating with a massive glass enclosure. It was found that cooker operation, with a load ratio of 4 kg of water per m^2 of maximum collecting area, with a glass lid on the pot provides 73.9 W, a value that is 46% greater than the power value obtained with black lid. Ebersviller and Jetter [14] have tested three designs of solar cookers by following strictly the protocol of the standard. The parabolic cooker, panel cooker and box cooker were tested side by side by using the load ratio recommended by the standard, i.e., 7 kg m^{-2}. The standardised power values obtained for the smaller cooker, HotPot panel cooker, and for the bigger cooker, parabolic SK14 cooker, were 25 W and 198 W, respectively. The difference between these two power values is very big. Chandak et al. [15] have done only one experiment to test side by side two different parabolic cookers with similar aperture area but adopting a smaller load ratio than the recommended by the standard. The duration of the experiment was only 1800 s. The power value obtained for the PRINCE15 cooker is around 9% greater than the value obtained for the SK14.

Mekonnen et al. [16] manufactured and tested a parabolic solar cooker under the Ethiopian climate with and without load were. The load tests have shown that the cooking power and the standard cooking power were 635 W and 375.8 W, respectively.

The recommended load ratio of the standard, 7 kg m^{-2}, is a relatively high value that does not represent what happens in real cooking operation in most of common solar cookers. For cooking under this specific recommended, a cooking set larger than the ones usually used in practice in case of most cookers is required and the cooking time would be too long. Moreover, when the weather conditions are not favourable,

Fig. 2. Solar cookers CSR1 and CSR2 being tested, respectively, without and a trivet.

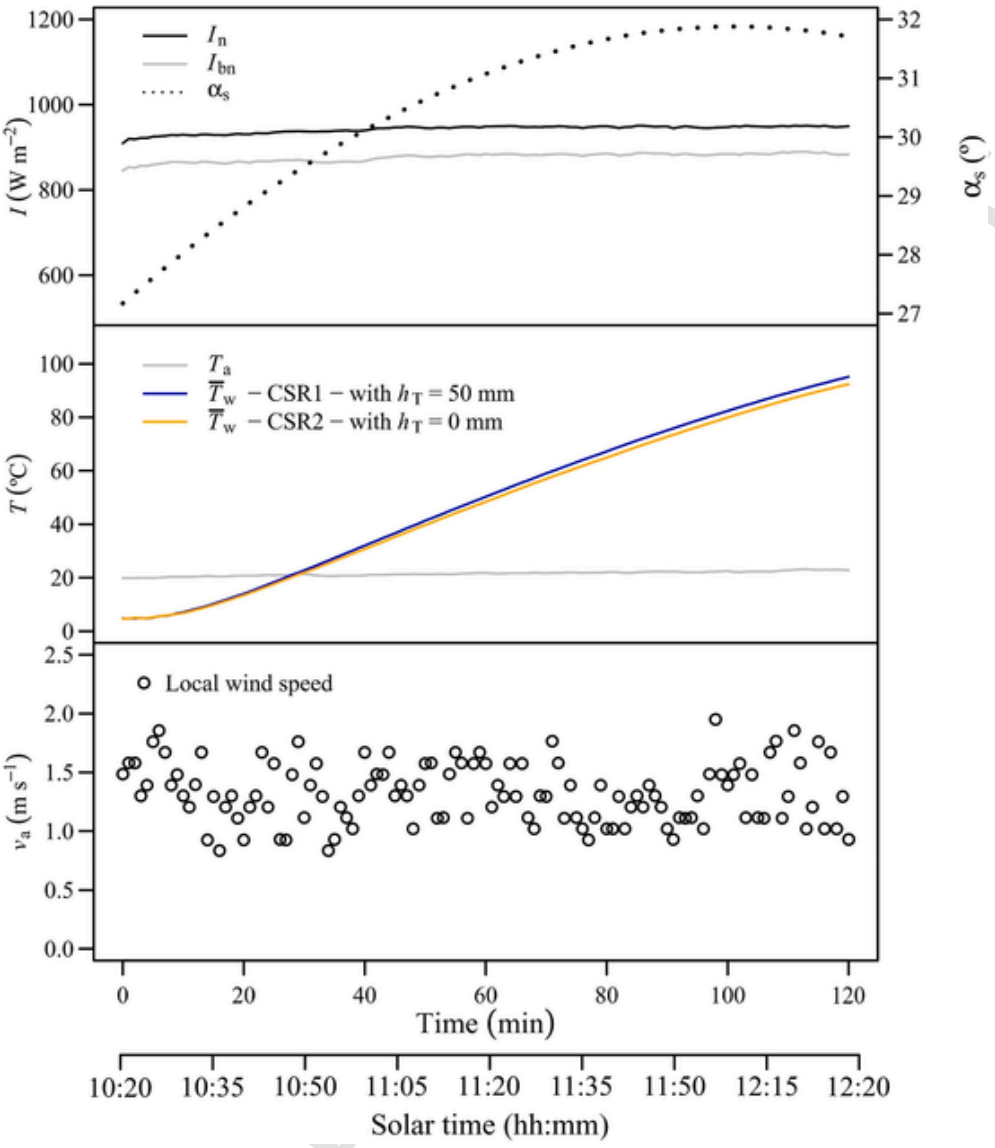

Fig. 3. Registered data of the exp. no. 52A, for the cooker CSR1 with a 50 mm height trivet (T50) and for the cooker CSR2 without trivet.

Table 1
Summary of the results of all tests carried out with different trivets.

Trivet	T0	T25	T50	T75	T100
h_T (mm)	0	25	50	75	100
n_t / n_{t1} / n_{t2}	14/4/10	8/3/5	13/7/6	7/4/3	5/3/2
n_p	93	50	90	53	37
$\dot{Q}_{S,0}$ (W)	104.8	106.3	107.5	108.0	106.9
a (W °C^{-1})	−0.584	−0.479	−0.566	−0.617	−0.584
R^2	0.733	0.623	0.709	0.752	0.929
$\dot{Q}_{S,50}$ (W)	75.6	82.3	79.3	77.1	77.7
$\dot{Q}_{S,50,CI95\%}$ (W)	(74.2,76.9)	(80.5,84.1)	(77.8,80.7)	(75.1,79.1)	(76.6,78.8)
$\dot{Q}_{S,50,PI95\%}$ (W)	(63.2,88.0)	(69.5,95.1)	(66.3,92.2)	(63.9,90.3)	(71.6,83.9)

the cooking success is questionable, because the maximum temperature is relatively low, and there is risk of bacteria development. Thus, the tests conducted by Ruivo et al. [13] and by Chandak et al. [15] can be seen as representing well the real cooking practice.

Lahkar et al. [17] have also tested side-by side a parabolic cooker SK14 and a box cooker in order to estimate the opto-thermal ratio parameter of each cooker. Similar investigation by testing side by side a box cooker and PRINCE15 parabolic cooker was performed by Sagade et al. [18] by using water and also ethylene glycol and glycerine as load and by Sagade et al. [19] by using only glycerine. Vengadesan and Senthil [20] have performed experiments with a box cooker for investigating the impact of using a finned cooking vessel. The different configurations of the cooking vessel were tested simultaneously in the same box cooker.

Kurt et al. [21] have investigated the performance of a box solar cooker by measuring the absorber plate, enclosure air and pot water temperatures and also using an artificial neural network to predict the same variables. Coccia et al. [22] have tested a powerful box cooker using peanut oil was. This study shows that, for the conditions of the test, the maximum power of the cooker occurs when the difference between the load temperature and the ambient temperature is about 60 °C, i.e., not far from the difference of 50 °C used in the definition of the standardised value adopted in reports following the standard protocol [12]. More recently, Tawfik et al. [5] have designed and tested a promising solar cooker that may be important to attract more people for cooking with solar energy. The thermal performance of the new design, equipped with a tracking-type bottom parabolic reflector, was estimated using glycerine as load and also without using any load.

Kumar [23] investigated the top thermal losses of box type solar cooker from heating characteristic curves. Indoor and outdoor experi-

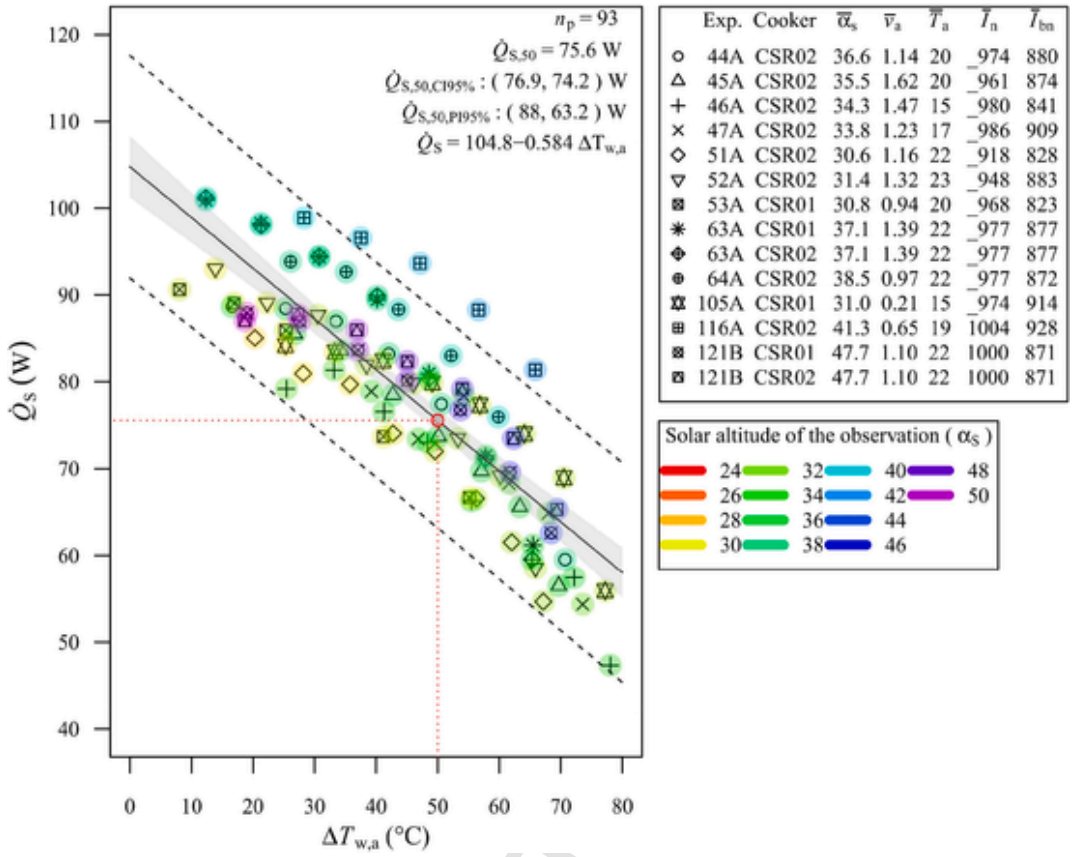

Fig. 4. Standardised power of all tests with trivet T0.

ments were performed to develop a correlation for the heat transfer coefficient as a function of pot water temperature, wind speed and ambient air temperature.

Collares-Pereira et al. [24] proposed procedures for testing solar box cookers requiring minimal investment by using cheap, simple and accessible test instruments for performance comparison of solar box cookers.

Al-Soud et al. [25] designed, constructed, operated and tested a parabolic solar cooker with automatic sun tracking system to avoid user manual tracking and user standing in the sun. The authors pointed out that i) the associated electromechanical setup is simple which reduces cost, maintenance and the possibility of failure and ii) the solar cooker is able to cook different kinds of food.

Kumaresan et al. [26] studied the performance of an indirect solar cooking system with a thermal energy storage tank a positive displacement pump and a double walled cooking unit using as the heat transfer fluid therminol 55 and D-Mannitol.

Saxena et al. [27] conducted an experimental research to investigate the thermal performance of a box cooker equipped with solar collector tubes filled with a heat storage media to speed up the cooking process and also to guarantee that the cooking process during periods of low or intermittent solar radiation. According to the findings of this work, the modified cooker is a low-cost cooker having a better performance than a conventional solar box cooker.

Bhave and Kale [28] designed and tested a cooking device using a eutectic mixture in a well-insulated container able to successfully store thermal energy at a melting point of 220 °C for indoor cooking like frying.

The standard establishes the maximum and the minimum values of the different uncontrolled weather variables to ensure that the repeatability of the obtained results is guaranteed. However, when minor changes in design of a particular cooker, in design of the cooking set or when two cookers with similar performance are being investigated, the standard protocol does not provide enough accurate results that are needed to evaluate the effect of those minor changes and to make the comparison of performance of different solar cookers.

When investigating minor changes in the design that can be associated with the properties of the reflector or to properties or elements of the cooking set, it is imperative to make experiments by testing two or more cookers side by side. A first set of experiments must be performed by using the same components in each cooker, i.e., without making any system design change, to ensure that all reference systems being tested are identical. After that, experiment is repeated by testing the systems side by side, where one system is tested again under the reference configuration and other systems are tested with the change in design to be investigated. By following this testing methodology, the uncontrolled variables of the experiment are the same in all systems being tested. For increasing the precision of this new approach here, proposed and investigated, the experimental data is processed by following a new procedure based on the analysis of the differences between the power values associated with each system. In present study, the R software tool was used for data processing and performing statistical analysis [29].

Conventional kitchen hobs, powered by gas, electricity, or wood, deliver thermal energy mainly to the bottom of the cooking vessel. The same is true of some solar cookers, particularly shallow parabolic concentrator solar cookers. However, box cookers, panel cookers, and deep parabolic cookers, deliver a significant part of the solar energy to the wall and to the lid of the cooking pot. When using a trivet, with an optimum height, to support the cooking set in a funnel cooker, it is expected that the delivered solar energy to the bottom of the pot would be higher than the scenario without using any trivet.

In present study, a new approach based on experimental results of testing two cookers side by side tests is adopted to evaluate the impact of using different height trivets on the power of the same prototypes of

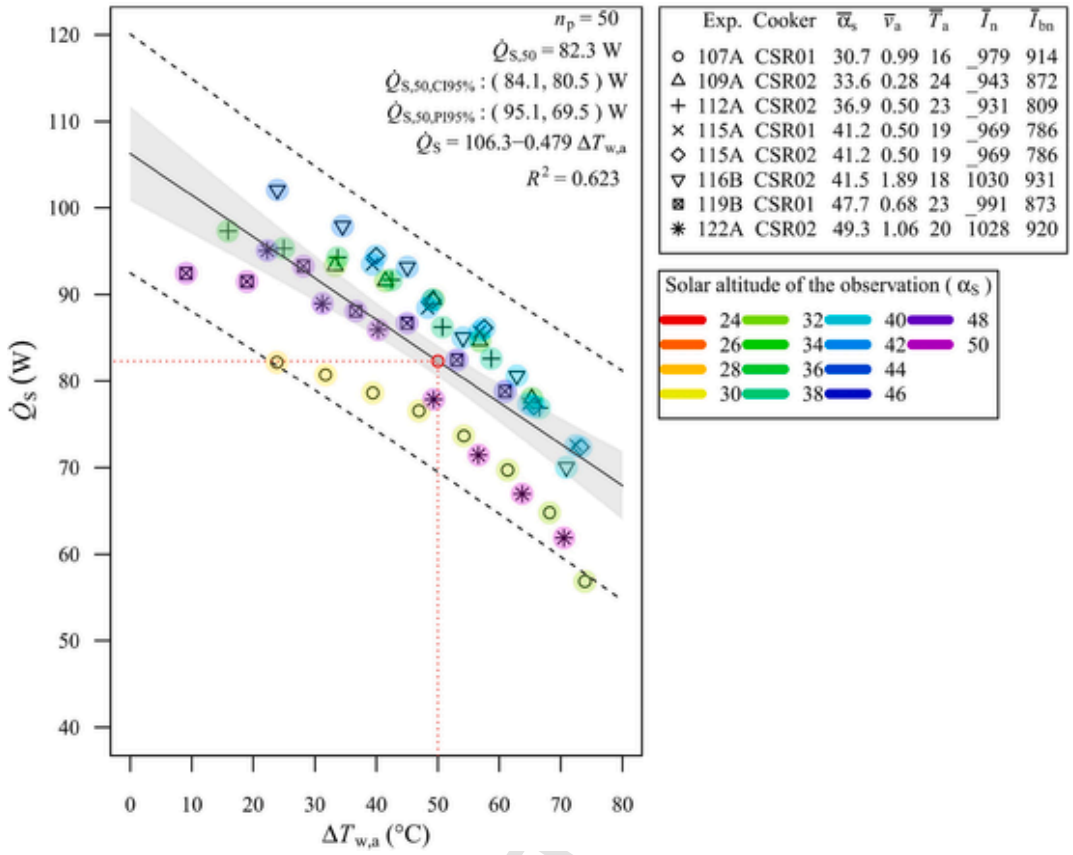

Fig. 5. Standardised power of all tests with trivet T25.

funnel solar cooker that were studied by Ruivo et al. [13]. The new approach adopts a time interval of 1 min for calculating the power instead of using the 10 min time interval recommended by the standard [12] and a curve fitting based on the LOESS adjustment for the evaluation of the difference in power values provided by different trivets. Tests of heating up 2 kg of water inside a black pot with a massive glass enclosure were carried out without using any trivet as done in previous work [13] and also using four trivets with heights of 25, 50, 75 and 100 mm.

According to authors' knowledge, this important and practical aspect has not yet been investigated and published in scientific literature.

2. Experimental set-up and instrumentation

Fig. 1 shows the solar cooker prototype composed of a funnel shape reflector, a base in extruded polystyrene and the cooking set over a trivet. The experimental set-up used by Ruivo et al. [13] is here adopted but now using also a trivet, new element being investigated, with different height values. The trivet is positioned in the centre of the square defining the cooking zone. The cooking set can be seen as the receiver of the system and it is composed by the pot and the glass enclosure. The base of the cooker is a rectangular piece of extruded *polystyrene* with a thickness of 80 mm. It is placed underneath the bottom the reflector to avoid direct contact between the reflector and the patio floor. Some tests were conducted by placing the cooking set directly onto the reflector surface of the cooking zone surface without any trivet and other tests were conducted by using trivets to support the cooking set at different heights: 25, 50, 75 and 100 mm. The mass values of the trivets range from 0.039 to 0.070 kg.

Two prototypes with the funnel reflector shape, CSR1 and CSR2, were tested side by side as depicted in Fig. 2. In this particular experiment, the cooker CSR2 is being tested with a trivet having 100 mm height and cooker CSR1 is being tested without trivet.

The two solar cookers have identical polished aluminium reflectors. Each cooker has a maximum collecting area of 0.50 m^2. A black enamelled steel pot, with an approximate capacity of 3 L and a mass of 540 g, was used in each cooking set. Each pot was covered with a glass lid having a mass of 366 g. Each set, pot and lid, was placed inside a massive glass enclosure composed of two windows of cloth washers. The mass values of the enclosure used in cooking set of cookers CSR1 and CSR2 were 2250 g and 2207 g, respectively. The difference between the mass values and shapes of the two enclosures are negligible. More details about the reflectors and components of the cooking set can be found in previous research work [13].

The sensor extremities of T-type thermocouples having an uncertainty of ±1 °C were placed in different positions inside the pot to measure the water temperature, being the average value considered as the representative value of the average temperature of water ($\bar{T}_w$) that was used in the calculations.

The ambient temperature and the wind speed were measured and logged every minute with sensors of an Onset weather station located near the solar cookers as can be seen in right part of Fig. 2. The uncertainty associated with measurement of the ambient temperature is ±0.2 °C.

Global solar irradiance in the plane normal to the beam solar radiation is required by the testing protocol of the ASAE S580.1 standard. In this work, it was found convenient to compute it through the Liu Jordan isotropic sky model [30], using data from global solar irradiance measured by two Hukseflux LP02 pyranometers, one in a horizontal plane and other in a titled plane that makes an angle of 50° with the horizontal. The two pyranometers are fixed to the same support, which was azimuthally adjusted every 20 min. The sensor uncertainty of each pyranometer is less than 1.8%. In the calculation procedure of the global solar irradiance in the plane normal to sun rays, the albedo was assumed to be 0.2, and the diffuse fraction of global horizontal radiation was got

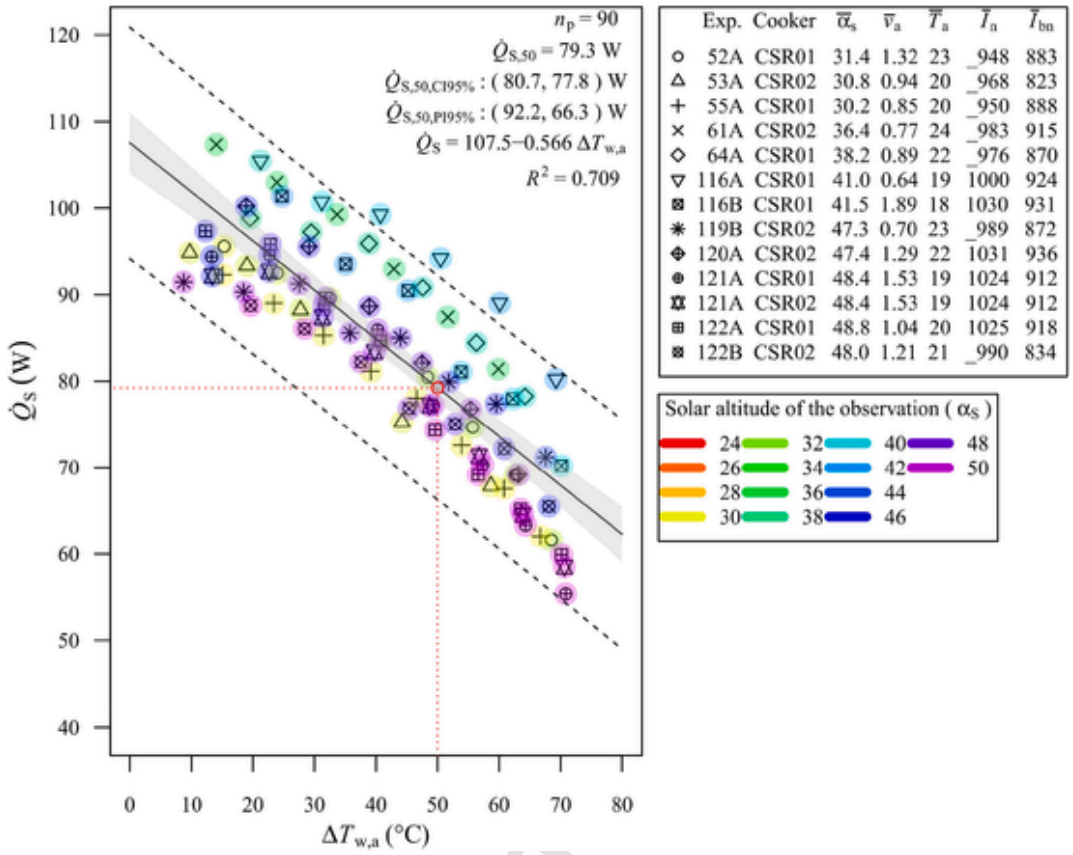

Fig. 6. Standardised power of all tests with trivet T50.

from measurements of a special device, a SPN1 Sunshine Delta-T Devices Pyranometer located in another nearby meteorological station. The global solar irradiance in the plane normal to the beam solar radiation could be measured alternatively by only a pyranometer if a continuous sun tracking system with both tilt and azimuth adjustments were adopted.

The load temperature measured by the thermocouples and the solar irradiance measured by the pyranometers were logged every 15 s by a Campbell Scientific CR1000 data logger. The mean value of each variable was calculated for every minute for subsequent calculations.

The experiments were carried out on the rooftop patio of the "Escuela de Ingenierías Industriales" at the University of Malaga, Spain, at latitude 36.9° N in two different periods, i.e., between November 2019 and February 2020 and between January and March 2021. During each test period, only azimuth adjustments of the both solar cookers and of both pyranometers were performed every 20 min. No tilt adjustments were performed. Some details of the instrumentation equipment used can be found in previous work of the authors [13].

3. Standard procedure of cooker performance analysis

A standard procedure adopted for analysing the performance of a solar cooker is recommended by standard ASAE S580.1 [12], which provides a protocol that allows comparing the power of different solar cookers designs. It also allows to investigate the changes in cooker power due to design changes of a particular cooker, as it is the case of being addressed in present study, since the changes on the power associated with designs changes are significant [13].

3.1. Test protocol

The standard procedure determines the conditions of testing a cooker and it also determines the valid ranges for the uncontrolled meteorological variables [12]. Some experiments carried out in present study do not fulfil strictly the conditions recommend by the standard because they were performed in cold months where the registered values of outside ambient temperature were below 20 °C and the average registered wind speed exceeded the value of 1 m s^{-1}.

The procedure of standard was intended mainly for testing box-type solar cookers [12], but it has been applied by others teams for testing parabolic dish cookers, panel cookers and evacuated tube based solar cookers [31,32]. In some cases, the testers have adopted the relatively high load ratio recommended by the standard, i.e., 7.0 kg m^{-2}. In other cases, testers have adopted a lower ratio value [13,15]. The solar cooker having multiple flat reflectors with funnel shape being investigated in present study can been as a panel solar cooker. Both funnel cooker prototypes were tested with a load ratio of 4.0 kg m^{-2}. The same load ratio value was considered by Ruivo et al. [13]. It is important to point out that the standard load ratio is not representative of the mass load being adopted in most cooking operations by most of the users when using a funnel cookers and also other types of cookers. Cooking operations with a load ratio of 7.0 kg m^{-2} in practice is very sporadic. The capacity of pots used in practice is not large enough or pot are used most of the times at partial load.

The test protocol of indicates the importance of plotting different variables in time series format as those represented in Fig. 3, that were recorded with an interval of 1 min during the experiment no. 52A performed on November 29, 2019. In this experiment, the cooker CSR1 was tested with a 50 mm height trivet and the cooker CSR2 was tested without trivet. This experiment started at 10:20 a.m. (solar time), with 750 g of ice and 1250 g of water in each pot. It enables to achieve more

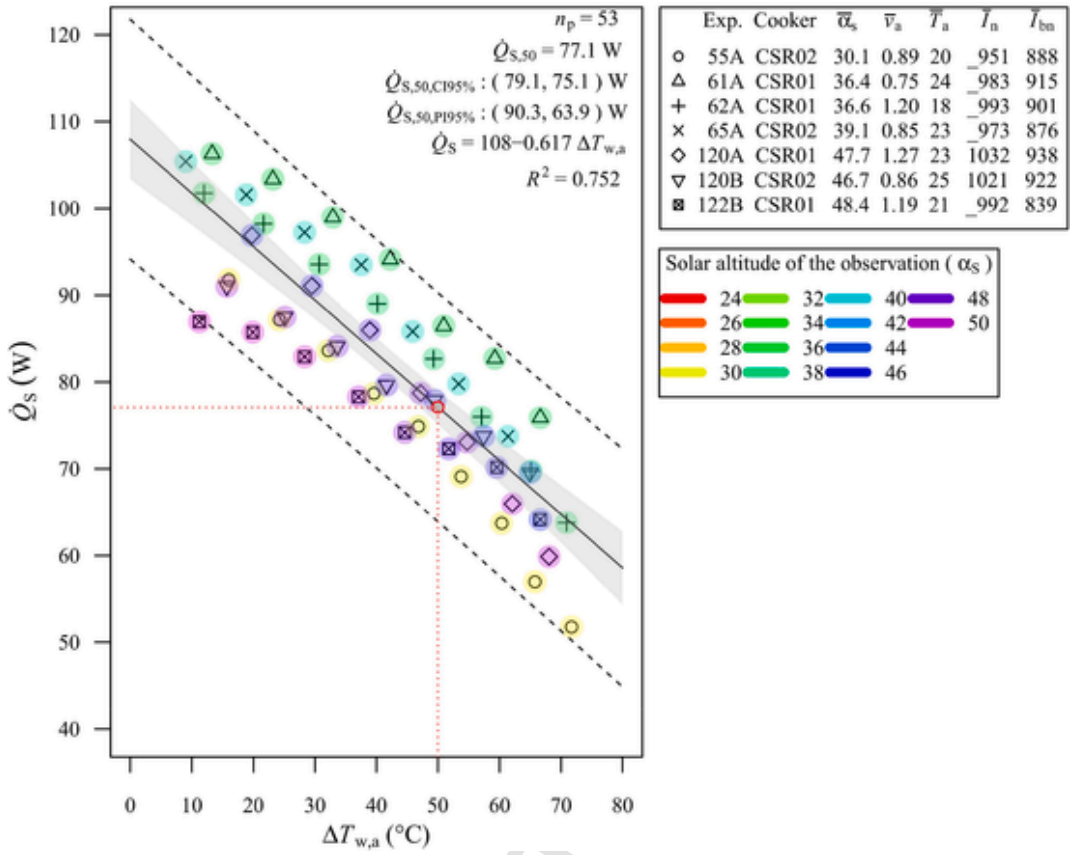

Fig. 7. Standardised power of all tests with trivet T75.

valid observation points than using only water, as demonstrated by Ruivo et al. [13]. The upper part of Fig. 3 shows the global normal solar irradiance I_n, i.e., the global solar irradiance on the plane perpendicular to the sun rays, the beam normal solar irradiance I_{bn} and the solar altitude angle α_s. The middle part depicts the ambient air temperature T_a and the water temperature $\bar{T}_w$ in cooking sets of both cookers CSR1 and CSR2. The lower part of Fig. 3 shows the 1 min average wind speed $\bar{v}_a$. This graphical treatment was done for all performed experiments.

3.2. Data processing for determining the cooking power

The ASAE S580.1 [12] standard determines a methodology to process the data acquired through the test protocol to determine the power of a solar cooker. Using the recorded values of T_a and $\bar{T}_w$ during one test spaced by a time interval of, Δt_i , 600 s, the corresponding increase temperature $\Delta T_{w,i}$ observed in the load, the power is calculated for each time interval *i* by Refs. [12,13]:

$$\dot{Q}_i = \frac{m_w c_w \Delta T_{w,i}}{\Delta t_i} \tag{1}$$

where c_w and m_w are constant values of the specific heat and mass of water, respectively. The specific heat is assumed constant because its dependence on temperature is very small. The mass of water is also assumed constant because there is no boiling phenomena and the amount of evaporated water scaping the pot during the test is assumed negligible.

The standard introduced the value of 700 Wm^{-2} for the global normal solar irradiance $I_{n,i}$ to normalise the radiation data measured during tests of a particular cooker carried out on different days with different and variable solar irradiance. Then, the standardized power is calculated for each time interval by Refs. [12,13]:

$$\dot{Q}_{S,i} = \dot{Q}_i \frac{700}{I_{n,i}} \tag{2}$$

and plotted as a function of the difference between $\bar{T}_w$ and T_a, which is represented by $\Delta T_{w,a}$. When applying the standard procedure, at least 30 valid points are required. This recommendation results on the need of performing several tests on different days. Using the plotted data, the following linear regression is determined to represent the relationship between the power $\dot{Q}_S$ and the difference $\Delta T_{w,a}$ as [13]:

$$\dot{Q}_S = \dot{Q}_{S,0} + a\Delta T_{w,a} \tag{3}$$

The standard specifies that the coefficient of determination R^2 associated with the regression line must be greater than 0.75. Based on this linear regression, the standard establishes the power $\dot{Q}_{S,50}$, which corresponds to $\Delta T_{w,a} = 50$ °C. It is used as the comparison parameter between solar cookers.

The prediction intervals $\dot{Q}_{S,PI95\%}$ and confidence $\dot{Q}_{S,CI95\%}$, not recommended by the standard, are also used in this study. These cooking parameters are statistical parameters that determine the uncertainty of the linear regression as established and investigated by Ruivo et al. [13].

3.3. Discussion of results of testing funnel cookers with different trivet heights

In practice of real cooking with funnel cooker shape here investigated, it is observed that most of the users do not use any trivet to raise the cooking set and that this aspect was not yet investigated. So, the impact of using a trivet is now investigate to better understanding how the performance of the cooker can be improved and to find the optimum height of the trivet when using a cooking set with massive glass enclo-

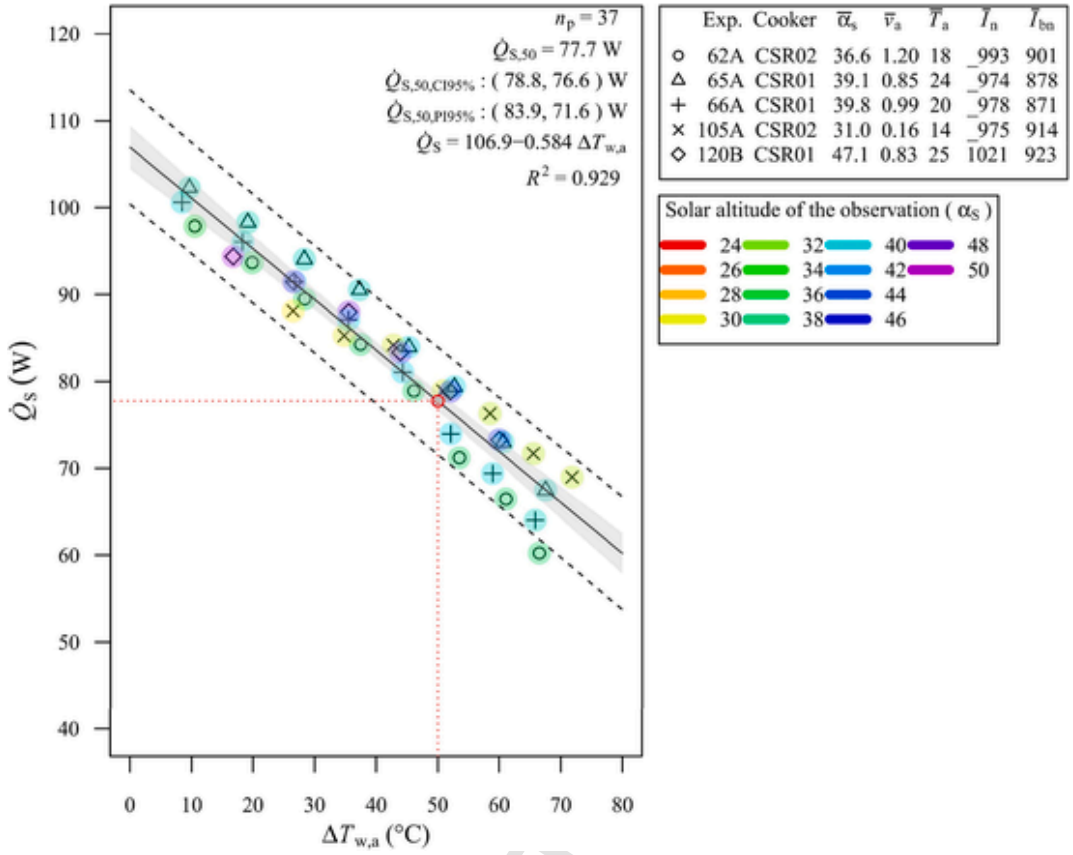

Fig. 8. Standardised power of all tests with trivet T100.

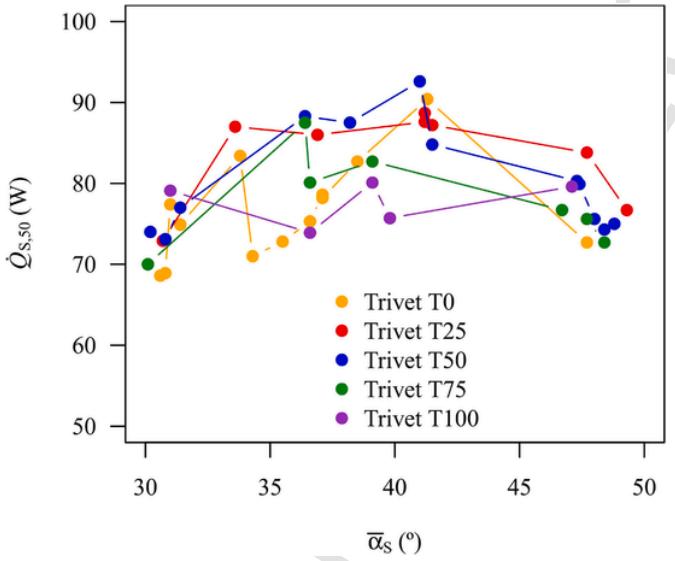

Fig. 9. Plots of standardised power $\dot{Q}_{S,50}$ for all tests.

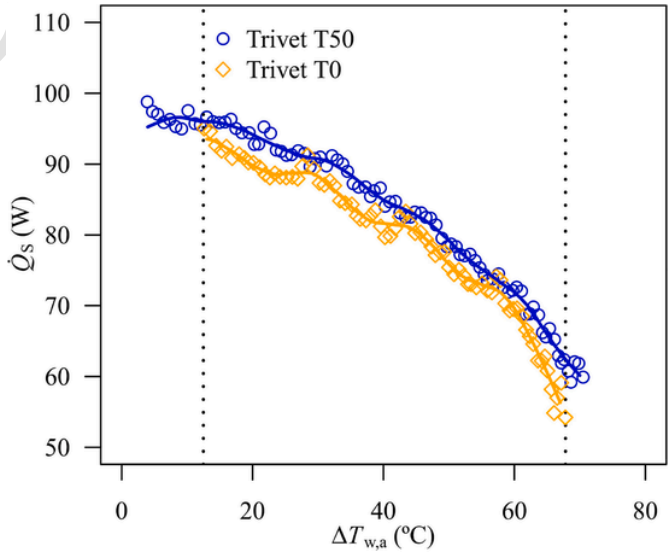

Fig. 10. Plots of standardized power and curve fittings, obtained with data of exp. no. 52A, for cooker CSR1 with trivet T50 and cooker CSR2 with trivet T0.

sure. By using a suitable trivet, it is expected to observe and increasing in the optical efficiency because reflected rays are also intercepted by the bottom of the cooking set. Moreover, conduction heat losses due to the direct contact of the cooking set with the reflector in the cooking zone of the cooker are eliminated.

A set of 47 tests were carried out in different 24 days for investigating specifically the influence of the height of the trivet on the performance of the funnel cooker. The data of the large number of tests are listed in Appendix A.

Table 1 and Figs. 4–8 present a summary of results of all test, including data related with the linear regression for each trivet, i.e., for trivets T0, T25, T50, T75 and T100.

By observing data depicted in legend of Figs. 4–8, it can be seen that the average solar altitude angle of all conducted tests ranges from 30° and 50°. The central axis of each solar cooker forms an angle of 38° with each rectangle reflector of the cooker [13].

When the solar funnel cooker tracks the sun perfectly, the sun rays are parallel to the central axis of the cooker. In this perfect operation,

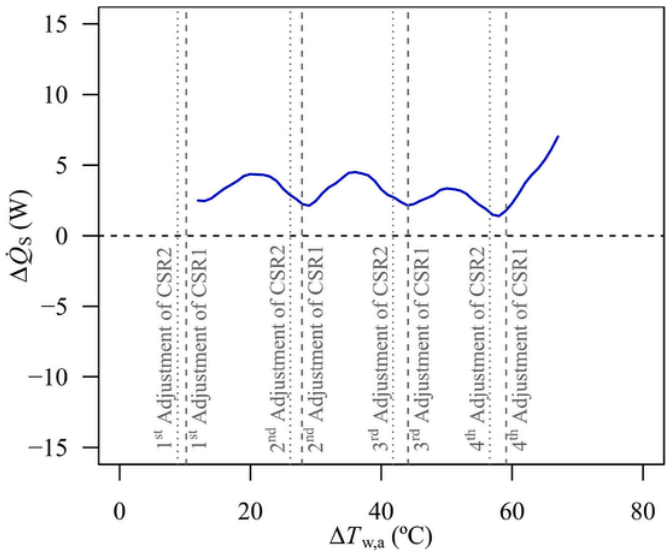

Fig. 11. Plot of $\Delta\dot{Q}_S$ of exp. no. 52A.

Table 2
Tests considered for side by side data processing for verifying identicalness of cooker designs (Configuration SSCAL).

h_T (mm)	0	0	0	0	25	25	50	50
Expt. no.	63A		121B		115A		121A	

Table 3
Tests considered for side by side data processing for evaluating change designs.

Configuration	SS50/0		SS25/50		SS75/50		SS100/75	
h_T (mm)	50	0	25	50	75	50	100	75
Expts. no.	52A, 53A, 64A, 116A		116B,119B, 122A		55A, 61A, 120A, 122B		62A, 65A, 120B	

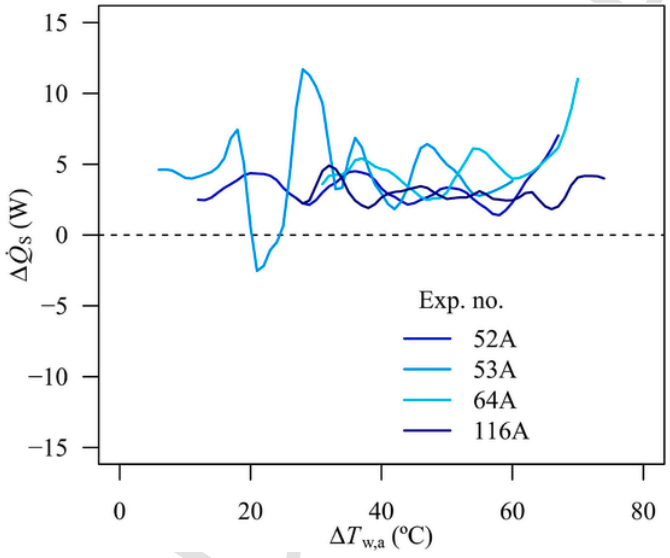

Fig. 12. Plots of $\Delta\dot{Q}_S$ for experiments of configuration SS50/0.

the aperture area of the cooker assumes its maximum value. Figs. 4–8 use a colour palette to identify the solar altitude angle (α_s) of each observation point.

Figs. 4–8 show that the power values depends significantly on the solar altitude angle. The greater values of the power occur when the solar altitude angle is close to 38°, i.e., points represented by clear blue colour. The smaller values of the power occur when the solar altitude angle is around 30°, i.e. points represented by yellow colour and when the solar altitude angle is around 50°, i.e. points represented by purple colour. Regarding the R^2 values of the linear regressions plotted in Figs. 4–7, it is observed that the values are smaller or close to 0.75, i.e., the limit recommended by the standard. On the other hand, the value of the regression depicted in Fig. 8 fits well in standard recommended range. In this figure, it can be seen that the impact of the solar altitude angle on the power is lower when a 100 mm height trivet is used. For better investigating the reason that power does not depend significantly on the solar altitude angle when using a 100 mm height trivet future research based on optical ray tracing analysis is being planned.

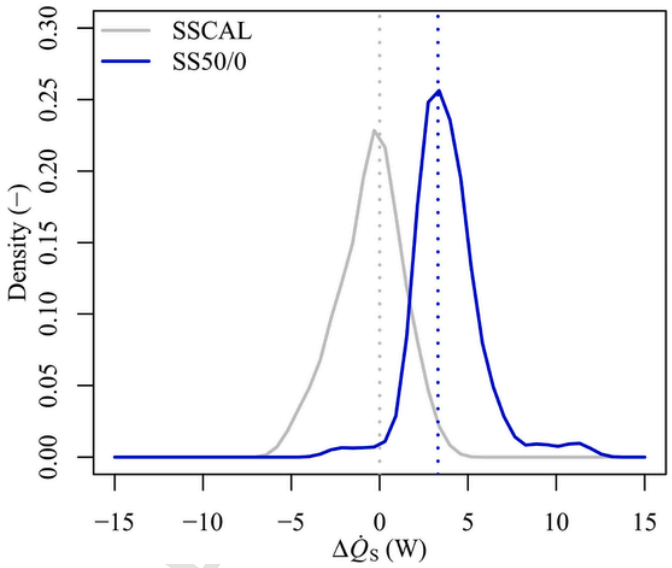

Fig. 13. Density plots of $\Delta\dot{Q}_S$ for experiments with configurations SSCAL and SS50/0.

For a better comparison of design changes being investigated, tests should be done in a narrow range of solar altitude angle, as was done by Ruivo et al. [13]. Following this strategy, better conclusions on the impact of different height trivets on the power of solar cookers can be extracted.

Fig. 9 depicts the power values of $\dot{Q}_{S,50}$ of all performed tests as a function of the average solar altitude angle for the five investigated configurations. It can be observed that cases with $\bar{\alpha}_s$ around 40°, the power of the solar cooker is greater than the power when $\bar{\alpha}_s$ is around 30° or 50°. For tests performed with $\bar{\alpha}_s$ around 40°, it is not possible to identity the trivet height that provides the greater power. For example, the two tests performed with trivet T50 with $\bar{\alpha}_s$ around 40° provide the highest and lowest $\dot{Q}_{S,50}$ values. The same phenomenon is verified for $\bar{\alpha}_s$ around 30° when using trivet T0.

The improvement of the power associated with the use of a trivet is small when compared to the improvement of 46% obtained when using a glass lid instead of using a metal lid [13]. The standard establishes the ranges of values for the different uncontrolled variables involved in an experiment. However, when the power changes due to changes in design of a cooker are small, the existence of the uncontrolled variables does not allow the right assessment of a design change of the cooker, especially when changes in power are small.

4. Performance analysis procedure for investigating small cooker design changes

A suitable approach is here proposed to overcome the limitations of the standard procedure when small design changes are being investi-

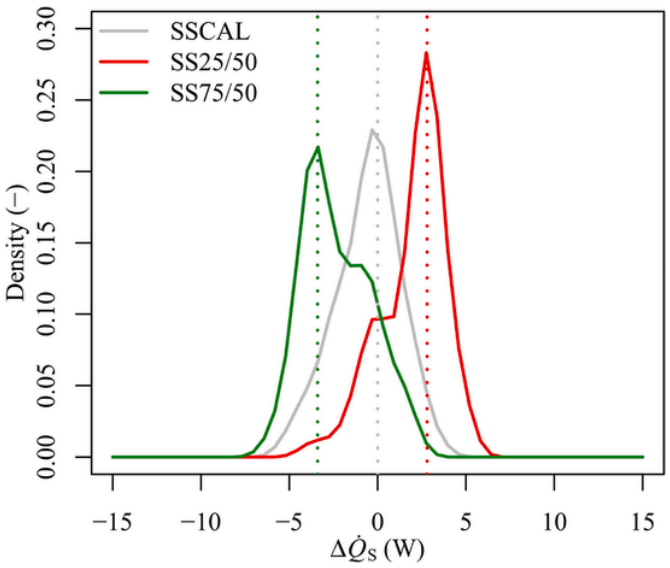

Fig. 14. Density plots of $\Delta\dot{Q}_S$ for experiments with configurations SSCAL, SS25/50 and SS75/50.

gated. It is supported by testing two or more identical cookers side by side, where one cooker has the reference design and the other cooker or other cookers are tested with only one design modification respecting the reference design. By following this side by side cooker testing approach, each cooker is tested under the same uncontrolled variables. Moreover, a proper and different protocol for data processing is adopted to increase the overall accuracy of the results.

4.1. Data processing for determining changes in cooking power

This section proposes a side by side testing approach that allows the evaluation of the power changes associated with modifications in design of cookers, mainly when the changes are relatively small. Some aspects of the ASAE S580.1 standard are taken into account in this new approach.

The data processing of this new approach uses the data obtained with the test protocol developed in section 3.1. The data processing associated with the standard protocol is summarized in section 3.2. The comparison of the performance of two cookers is performed by plotting the standardised power $\dot{Q}_S$ as a function of the difference $\Delta T_{w,a}$, by considering observation points spaced with a time interval of 600 s. The standard protocol recommends the use of a minimum of 30 observation points that must be collected imperatively from experiments conducted in two or more days. A linear regression is applied to the collected data and the value $\dot{Q}_{S,50}$ is used for comparison performance of different cooker designs. The standard approach is easy to use and provides accurate results only when the power values of the cookers tested are considerably different. Even the use of the linear regression enables the comparison of two $\dot{Q}_S$ values for a single $\Delta T_{w,a}$, it provides unfortunately a loss of the accuracy of the measured data.

In the new approach, here proposed, the data processing is improved in order to guaranty the accuracy of the output results. A first modification consists in considering more observation points that are spaced with a shorter time interval of 60 s. This consideration provides a better plot resolution of the relationship between the power values $\dot{Q}_S$ and the difference $\Delta T_{w,a}$. The power is calculated with Eq. (2). A second modification consists in using a curve fitting for the plot of each cooker design because, even the observation points are recorded at the same time, the registered difference $\Delta T_{w,a}$ is not the same in both cookers. Thus, to compare the power values of each cooker for the same $\Delta T_{w,a}$, a suitable curve fitting based on the loess adjustment is done [33], which allows the calculation of the difference between two curves. The loess adjustment is a local polynomial regression fitting and smoothing procedure.

As example, Fig. 10 depicts the all observation points applying the new approach for experiment no. 52A, where the CSR1 was tested with trivet T50 and the CSR2 without trivet (T0). It shows also the two curve fitting curves obtained with loess adjustment. The increase in power due to the use of the trivet is evident, but to assess more accurately way, the difference of standardized powers given by the two curves, here called $\Delta\dot{Q}_S$, is adopted. This approach provides information across the entire $\Delta T_{w,a}$ range instead of using only the $\dot{Q}_{S,50}$ recommended by the standard procedure. Fig. 10 also shows the range of $\Delta T_{w,a}$ values, defined by the two vertical lines, where there are points for both plots. The differences $\Delta\dot{Q}_S$ calculated for this range are represented in Fig. 11 as a function of $\Delta T_{w,a}$ together with the impact of making the azimuth adjustments in each cooker each 20 min. From both Figs. 10 and 11, $\Delta\dot{Q}_S$ does not present a monotonic dependence of $\Delta T_{w,a}$. The improvement caused by using a trivet T50 seems to be similar at high, medium and low values of $\Delta T_{w,a}$ because the use of the trivet affects mainly the optic efficiency of the cooker.

In Fig. 11, the evolution of $\Delta\dot{Q}_S$ shows a periodic behaviour that is associated with the periodic slope change of the curves shown in Fig. 10. The vertical lines inserted in Fig. 11 represent the instants of azimuth adjustments of CSR1 and CSR2 each 20 min. It is verified that the period of oscillatory behaviour of the curve is related with the period of cookers adjustments. An optical raytracing analysis and a study supported by results of testing different cooker designs with an intermediate temperature fluid are being conducted for better investigating how the standardised power plots in some cooker designs do not exhibit a perfect linear trend.

4.2. Discussion of results of testing funnel cookers with different trivet heights

A set of 18 experiments has been carried out in 13 days to analyse the impact of the trivet's height on the power of the funnel cooker. Tables 2 and 3 lists the five configuration of the experiments that were performed. Each configuration was repeated three times as minimum. The detailed information of each experiment is listed in Appendix A and plotted in Figs. 4–8.

The SSCAL configuration corresponds to experiments conducted with cookers using the same trivet height or without using any trivet in both cookers being tested at the same time. The experiments conducted with SSCAL configuration can be seen as calibration procedure that were performed just to investigate if each cooker tested side by side provides identical performance results for cases of using trivet with height of 25 mm, 50 mm and case without trivet.

Some pairs of values of height trivet associated with configurations SS50/0, SS25/50, SS75/50 and SS100/75 listed in Table 3 were tested. Each configuration can be represented generically by SS*Ti*/*Tj*. For each configuration tested the difference of power is evaluated by:

$$\Delta\dot{Q}_S = \dot{Q}_{S,Ti} - \dot{Q}_{S,Tj} \tag{4}$$

where $\dot{Q}_{S,Ti}$ and $\dot{Q}_{S,Tj}$ are the standardised power values of cooker with trivet *Ti* and trivet *Tj*, respectively. Both trivets *Ti* and *Tj* here investigate are T0, T25, T50, T75 and T100, which designations are associated with the respective height of the trivet 0, 25, 75 and 100 mm.

Fig. 12 depicts the plots of $\Delta\dot{Q}_S$ for all experiments conducted with configuration SS50/0, i.e., trivet T50 and without trivet (T0). The representation of the results by this format is very misleading in order to extract right conclusion about the influence of a design change. For this reason, density plot function is adopted for making graphs of Figs. 13–15. A density plot shows the distribution of data over a continuous interval instead of using the corresponding histogram data [34]. It uses

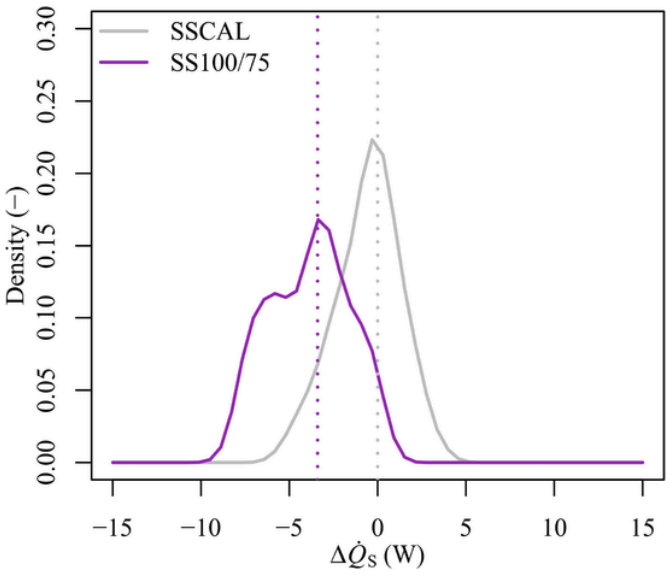

Fig. 15. Density plots of $\Delta\dot{Q}_S$ for experiments with configurations SSCAL and SS100/75.

a kernel smoothing out the noise and its peaks evidence where the values are concentrated over the interval.

The density plot associated with experiments of configuration SSCAL is represented in all Figs. 13–15 and also other density plots associated to other configurations listed in Table 3. The density plot of configuration SSCAL has a bell shaped centred around $\Delta\dot{Q}_S = 0$ W, which is an expected result that demonstrates the suitability of the new approach for investigating design changes of a cooker based on side by side experiments.

The density plots associated with configurations SS50/0 and SS100/75 are depicted in Figs. 13 and 15. The density plots associated with configurations SS25/50 and SS75/50 are depicted in Fig. 14.

From Fig. 13 it is observed that the curve of configuration SS50/0 is shifted towards $\Delta\dot{Q}_S = 3.3$ W. This result shows that the use of a 50 mm height trivet leads to an increase of the power of the funnel cooker by 3.3 W respecting the case without using any trivet.

Fig. 14 depicts the density plots of configurations SSCAL, SS25/50 and SS75/50. The results of the configuration SS75/50 indicated that $\Delta\dot{Q}_S$ values are grouped around $\Delta\dot{Q}_S = -3.4$ W, which means that power of the cooker with trivet T75 is smaller than the power of the cooker using trivet T50, in 3.4 W. This reduction in power is similar to the increase in power when using trivet T50 instead of using cooker without trivet (T0). So, the power of cooker with trivet T75 is similar to the power of the cooker without using any trivet (T0). The results of configuration SS25/50 show that $\Delta\dot{Q}_S$ are grouped around $\Delta\dot{Q}_S = 2.8$ W. Therefore, the use of trivet T25 improves the power of the solar cookers by 2.8 W when compared to the use of trivet T50. When comparing the performance between a cooker with trivet T25 and a cooker without trivet (T0), the performance gain is estimated to be around 6 W.

Finally, Fig. 15 presents the density plots for configurations SSCAL and SS100/75. The plotted results indicate that the $\Delta\dot{Q}_S$ values for the configuration SS100/75 are grouped also around the value of −3.4 W. It means that cooker operation with trivet T100 is less efficient than using the trivet T75 and it is also less efficient than cooker operation without trivet (T0).

From the analysis of density plots of all configurations investigated, it can be concluded that the optimum trivet height is 25 mm.

It is important to point out that all experiments conducted with the same configurations provide results with high reproducibility. For example, all experiments with configuration SS50/0 show that it is better to use a trivet T50 than not using a trivet (T0). It is also to point out that the $\Delta\dot{Q}_S$ values obtained are representative of the solar altitudes of the experiments carried out because the power $\dot{Q}_S$ depends on the solar altitude angle.

5. Conclusions

The ASAE S580.1 standard protocol is not appropriate to evaluate the impact of design modifications causing small changes in the power of the cooker, due to the influence of uncontrolled weather variables occurring on the different test days and also when solar altitude angle evolution differs from one experiment to another experiment. To overcome these problems, a more accurate approach based on a side by side experimental test analysis was proposed and used to investigate how the trivet height influences the power of the funnel cooker. Trivets with different heights, used to raise the cooking set having a massive glass enclosure, were tested. The height of trivet ranged from 0 to 100 mm.

The main findings of the present work are:

i) The new approach is based on the simultaneous experimental tests of two or more solar cookers. Thus, it allows to quantify minor and major design modifications of a particular solar cooker and also to quantify the performance of different cooker designs with a better accuracy.
ii) The new approach adopts a shorter time interval and a curve fitting based on the LOESS adjustment for each cooker design tested side by side for making the evaluation of the difference in power.
iii) Density plots are adopted in the new approach for analysing, more effectively, the experimental data subjected to noise.
iv) Several calibration experiments were performed by testing the two cookers side by side with the same trivet height, having been verified a good identicalness in the results.
v) Different design configurations with different heights of trivets were experimentally tested and compared in pairs of different heights of trivet.
vi) The new methodology is robust because the results of testing each configuration, at least three times, are convergent.
vii) The impact of any design change in the cooker power is detected by the new approach for any value of $\Delta T_{w,a}$. In case of a change in trivet height, the difference in power is approximately constant in all range of $\Delta T_{w,a}$ because this design change affects mainly the optical efficiency of the system.
viii) The trivet that provides greater power has a height of 25 mm. The difference between power obtained with the trivet height of 25 mm and the power obtained without using any trivet is around 6 W. The other trivet that provides a power gain, respecting the case of operation without a trivet, has a height of 50 mm, being the gain around 3 W.
ix) Cooker operation with 75 mm height trivet provides the same power as cooker operation without a trivet. Moreover, cooker operation with a 100 mm height trivet is detrimental because a loss of around 3 W in power is obtained respecting the operation without a trivet.
x) The standardised power variation was estimated to be around 10 W when changing trivet from the worse to the best height value.

Future research studies based on experiments carried out, being conducting and planned by the authors will be addressed. Testing the effect of using matte black pots, smaller and bigger pots and perfect sun tracking are some examples of studies that can be conducted also by applying the same new approach here used.

CRediT authorship contribution statement

Xabier Apaolaza-Pagoaga: Supervision, Conceptualization, Methodology, Formal analysis, Investigation, Data curation, Visualization, Writing – original draft, Writing – review & editing. **Antonio Carrillo-Andrés:** Conceptualization, Methodology, Formal analysis, Software, Data curation, Visualization, Writing – original draft, Writing – review & editing. **Celestino Rodrigues Ruivo:** Conceptualization, Methodology, Formal analysis, Writing – review & editing.

Declaration of competing interest

The authors declare that they have no known competing financial interests or personal relationships that could have appeared to influence the work reported in this paper.

Appendix A. Data of all tests conducted in the present study

Table A1 lists the data of the 47 tests carried out in 24 days for investigating the influence of different trivet heights on the standardised power of the cooker. The listed time values correspond to solar time. Some tests have started with water as load (LW) and other tests have started with mixture of ice and water (LIW).

Table A1
Data from experiments conducted with different height trivets.

Expt. no.	44A	45A	46A	47A	51A	52A	53A	63A
Cooker	CSR2	CSR2	CSR2	CSR2	CSR2	CSR2	CSR1	CSR1
Start time	10:34	11:02	10:30	11:03	9:30	10:20	10:58	11:39
End time	12:13	12:41	12:28	12:52	11:49	12:19	12:47	13:28
Date	Nov 6, 2019	Nov 12, 2019	Nov 15, 2019	Nov 18, 2019	Nov 28, 2019	Nov 29, 2019	Dec 4, 2019	Feb 10, 2020
Height of trivet (mm)	0	0	0	0	0	0	0	0
Load	LW	LW	LW	LW	LIW	LIW	LIW	LIW
n_p	6	7	8	6	8	8	5	7
$\bar{I}_n$ (W m^{-2})	974	961	980	986	918	948	968	977
$\bar{I}_{bn}$ (W m^{-2})	880	874	841	909	828	883	823	877
$\bar{\alpha}_s$ (º)	37	36	34	34	31	31	31	37
$\bar{T}_a$ (ºC)	20	20	15	17	22	23	20	22
$\bar{v}_a$ (m s^{-1})	1.1	1.6	1.5	1.2	1.2	1.3	0.9	1.4
$\dot{Q}_{S,50}$ (W)	75.1	72.8	69.1	74.3	68.9	73.4	69.9	77.5
$\dot{Q}_{S,0}$ (W)	102.5	105.2	100.1	106.3	99.6	104.1	97.2	114.4
a (–)	−0.55	−0.65	−0.62	−0.64	−0.61	−0.60	−0.55	−0.74
R^2	0.889	0.961	0.930	0.793	0.953	0.930	0.969	0.934
Expt. no.	63A	64A	105A	116A	121B	121B	107A	109A
Cooker	CSR2	CSR2	CSR1	CSR2	CSR1	CSR2	CSR1	CSR2
Start time	11:39	10:34	10:14	10:05	12:10	12:10	10:05	10:05
End time	13:28	12:03	12:05	11:29	13:46	13:46	11:58	11:45
Date	Feb 10, 2020	Feb 11, 2020	Jan 12, 2021	Feb 23, 2021	Mar 15, 2021	Mar 15, 2021	Jan 14, 2021	Jan 29, 2021
Height of trivet (mm)	0	0	0	0	0	0	25	25
Load	LIW	LW	LW	LW	LW	LW	LW	LW
n_p	7	6	8	6	7	7	8	5
$\bar{I}_n$ (W m^{-2})	977	977	974	1004	1000	1000	979	943
$\bar{I}_{bn}$ (W m^{-2})	877	872	914	928	871	871	914	872
$\bar{\alpha}_s$ (º)	37	39	31	41	48	48	31	34
$\bar{T}_a$ (ºC)	22	22	15	19	22	22	16	24
$\bar{v}_a$ (m s^{-1})	1.4	1.0	0.2	0.7	1.1	1.1	1	0.3
$\dot{Q}_{S,50}$ (W)	76.9	81.9	76.8	92.6	75.6	78.0	72.9	87.0
$\dot{Q}_{S,0}$ (W)	115.2	113.9	100.2	117.3	100.49	98.7	99.2	110.7
a (–)	−0.77	−0.64	−0.47	−0.49	−0.5	−0.41	−0.47	−0.47
R^2	0.932	0.932	0.802	0.949	0.923	0.860	0.904	0.927
Expt. no.	112A	115A	115A	116B	119B	122A	52A	53A
Cooker	CSR2	CSR1	CSR2	CSR2	CSR1	CSR2	CSR1	CSR2
Start time	10:05	11:12	11:12	12:00	12:00	10:10	10:20	10:58
End time	11:39	12:43	12:43	13:25	13:29	11:43	12:19	12:47
Date	Feb 11, 2021	Feb 18, 2021	Feb 18, 2021	Feb 23, 2021	Mar 11, 2021	Mar 12, 2021	Nov 29, 2019	Dec 4, 2019
Height of trivet (mm)	25	25	25	25	25	25	50	50
Load	LW	LW	LW	LW	LW	LW	LIW	LIW
n_p	7	5	5	6	7	7	8	5
$\bar{I}_n$ (W m^{-2})	931	969	969	1030	991	1028	948	968
$\bar{I}_{bn}$ (W m^{-2})	809	786	786	931	873	920	883	823
$\bar{\alpha}_s$ (º)	37	41	41	42	49	49	31	31
$\bar{T}_a$ (ºC)	23	19	19	18	20	20	23	20
$\bar{v}_a$ (m s^{-1})	0.5	0.5	0.5	1.9	1.1	1.1	1.3	0.9
$\dot{Q}_{S,50}$ (W)	86.0	87.6	88.7	87.2	83.8	76.7	77.0	73.1

Expt. no.	44A	45A	46A	47A	51A	52A	53A	63A
$\dot{Q}_{S,0}$ (W)	105.9	119.4	122.6	120.3	97.3	111.6	108.0	102.9
a (–)	−0.40	−0.64	−0.68	−0.66	−0.27	−0.70	−0.62	−0.59
R^2	0.934	0.973	0.972	0.960	0.851	0.990	0.961	0.976
Expt. no.	55A	61A	64A	116A	116B	119B	120A	121A
Cooker	CSR2	CSR2	CSR1	CSR1	CSR1	CSR2	CSR2	CSR1
Start time	10:44	10:40	10:34	10:05	12:00	12:00	10.10	10:10
End time	12:53	12:19	11:53	11:29	13:25	13:29	11.41	10:41
Date	Dec 10, 2019	Feb 3, 2020	Feb 11, 2020	Feb 23, 2021	Feb 23, 2021	Mar 11, 2021	Mar 12, 2021	Mar 15, 2021
Height of trivet (mm)	50	50	50	50	50	50	50	50
Load	LIW	LIW	LW	LW	LW	LW	LW	LW
n_p	9	6	6	6	6	8	6	7
$\bar{I}_n$ (W m^{-2})	950	983	976	1000	1030	989	1031	1024
$\bar{I}_{bn}$ (W m^{-2})	888	915	870	924	931	872	936	912
$\bar{\alpha}_s$ (º)	30	36	38	41	42	47	47	48
$\bar{T}_a$ (ºC)	20	24	22	19	18	23	22	19
$\bar{v}_a$ (m s^{-1})	0.9	0.8	0.9	0.6	1.9	0.7	1.3	1.5
$\dot{Q}_{S,50}$ (W)	69.9	88.3	87.5	92.6	84.8	80.3	79.9	75.6
$\dot{Q}_{S,0}$ (W)	105.5	116.5	110.7	117.3	118.1	97.4	115.1	113.8
a (–)	−0.71	−0.57	−0.46	−0.49	−0.67	−0.34	−0.70	−0.76
R^2	0.979	0.986	0.909	0.949	0.981	0.902	0.990	0.988
Expt. no.	121A	122A	122B	55A	61A	62A	65A	120A
Cooker	CSR2	CSR1	CSR2	CSR2	CSR1	CSR1	CSR2	CSR1
Start time	10:10	10:10	10:10	10:44	10:40	10:29	10:34	10.10
End time	10:41	11:43	11:49	12:53	12:29	12:28	12:23	11.41
Date	Mar 15, 2021	Mar 16, 2021	Mar 16, 2021	Dec 10, 2019	Feb 3, 2020	Feb 4, 2020	Feb 12, 2020	Mar 12, 2021
Height of trivet (mm)	50	50	50	75	75	75	75	75
Load	LW	LW	LW	LW	LIW	LIW	LIW	LW
n_p	6	8	7	9	7	8	7	7
$\bar{I}_n$ (W m^{-2})	1024	1025	990	951	983	992	973	1032
$\bar{I}_{bn}$ (W m^{-2})	912	918	834	888	915	901	876	938
$\bar{\alpha}_s$ (º)	48	49	48	30	36	37	39	48
$\bar{T}_a$ (ºC)	19	20	21	20	24	18	23	23
$\bar{v}_a$ (m s^{-1})	1.5	1	1.2	0.9	0.8	1.2	0.9	1.3
$\dot{Q}_{S,50}$ (W)	79.9	75.0	75.6	69.9	87.5	80.1	82.7	75.6
$\dot{Q}_{S,0}$ (W)	115.1	109.9	98.8	105.5	116.3	112.3	113.2	113.8
a (–)	−0.70	−0.70	−0.46	−0.71	−0.58	−0.65	−0.61	−0.76
R^2	0.990	0.974	0.978	0.979	0.977	0.978	0.972	0.988

Expt. no.	120B	122B	62A	65A	66A	105A	120B
Cooker	CSR2	CSR1	CSR2	CSR1	CSR1	CSR2	CSR1
Start time	12:10	10:10	10:29	10:34	10:44	10:14	12:10
End time	13:39	11:49	12:28	12:33	12:43	12:05	13:39
Date	Mar 12, 2021	Mar 16, 2021	Feb 4, 2020	Feb 12, 2020	Feb 14, 2020	Jan 12, 2021	Mar 12, 2021
Height of trivet (mm)	75	75	100	100	100	100	100
Load	LW	LW	LIW	LIW	LIW	LW	LW
n_p	7	8	8	8	8	7	6
$\bar{I}_n$ (W m^{-2})	1021	992	993	974	978	975	1021
$\bar{I}_{bn}$ (W m^{-2})	922	839	901	878	871	914	923
$\bar{\alpha}_s$ (º)	47	48	37	39	40	31	47
$\bar{T}_a$ (ºC)	25	21	18	24	20	14	25
$\bar{v}_a$ (m s^{-1})	0.9	1.2	1.2	0.9	1.0	0.2	0.8
$\dot{Q}_{S,50}$ (W)	76.7	72.7	73.9	80.1	75.7	79.1	79.6
$\dot{Q}_{S,0}$ (W)	98.2	93.2	107.3	110.3	108.0	100.7	104.1
a (–)	−0.43	−0.41	−0.67	−0.60	−0.65	−0.43	−0.49
R^2	0.993	0.976	0.981	0.982	0.988	0.977	0.978

References

[1] M. Aramesh, M. Ghalebani, A. Kasaeian, H. Zamani, G. Lorenzini, O. Mahian, S. Wongwises, A review of recent advances in solar cooking technology, Renew. Energy 140 (2019) 419–435, https://doi.org/10.1016/j.renene.2019.03.021.

[2] N.L. Panwar, S.C. Kaushik, Surendra Kothari, State of the art of solar cooking: an overview, Renew. Sustain. Energy Rev. 16 (2012) 3776–3785, https://doi.org/10.1016/j.rser.2012.03.026.

[3] E. Cuce, P.M. Cuce, A comprehensive review on solar cookers, Appl. Energy 102 (2013) 1399–1421, https://doi.org/10.1016/j.apenergy.2012.09.002.

[4] Solar Cookers International Solar cooker designs https://solarcooking.fandom.com/wiki/Category:Solar_cooker_designs s13 May 2021 Accessed

[5] M.A. Tawfik, A.A. Sagade, R. Palma-Behnke, H.M. El-Shal, W.E. Abd Allah, Solar cooker with tracking-type bottom reflector: an experimental thermal performance evaluation of a new design, Sol. Energy 220 (2021) 295–315, https://doi.org/10.1016/j.solener.2021.03.063.

[6] I. Edmonds, Low cost realisation of a high temperature solar cooker, Renew. Energy 121 (2018) 94–101, https://doi.org/10.1016/j.renene.2018.01.010.

[7] A.M. Khallaf, M.A. Tawfik, A.A. El-Sebaii, A.A. Sagade, Mathematical modeling and experimental validation of the thermal performance of a novel design solar cooker, Sol. Energy 207 (2020) 40–50, https://doi.org/10.1016/j.solener.2020.06.069.

[8] SK1.4 Solar cooking Wiki https://solarcooking.fandom.com/wiki/SK1.4 s12 May 2021 Accessed

[9] PRINCE-40 Solar cooking Wiki https://solarcooking.fandom.com/wiki/PRINCE-40 s12 May 2021 Accessed

[10] Sunoven https://sunoven.com s12 May 2021 Accessed

[11] F. Chacon, D. Baillie, D. Müller, P. Gießler, Hot stone cooking with an ultralight membrane solar concentrator, CONSOLFOOD 2018, Faro, Portugal, 22–24 January 2018.
[12] ASAE S580.1 NOV2013, Testing and Reporting Solar Cooker Performance, American Society of Agricultural Engineers, Michigan, USA, 2013.
[13] C. Ruivo, A. Carrillo-Andrés, X. Apaolaza-Pagoaga, Experimental determination of the standardised power of a solar funnel cooker for low sun elevations, Renew. Energy 170 (2021) 364–374, https://doi.org/10.1016/j.renene.2021.01.146.
[14] S.M. Ebersviller, J.J. Jetter, Evaluation of performance of household solar cookers, Sol. Energy 208 (2020) 166–172, https://doi.org/10.1016/j.solener.
[15] A. Chandak, S.K. Somani, P.M. Suryaji, Comparative analysis of SK-14 and PRINCE-15 solar concentrators, Proceedings of the World Congress on Engineering III, London, U.K, 2011, July 6–8.
[16] B.A. Mekonnen, K.W. Liyew, M.T. Tigabu, Solar cooking in Ethiopia: experimental testing and performance evaluation of SK14 solar cooker, Case Stud. Therm. Eng. 22 (2020) 100766, https://doi.org/10.1016/j.csite.2020.100766.
[17] P.J. Lahkar, R.K. Bhamu, S.K. Samdarshi, Enabling inter-cooker thermal performance comparison based on cooker opto–thermal ratio (COR), Appl. Energy 99 (2012) 491–495, https://doi.org/10.1016/j.apenergy.2012.05.034.
[18] A.A. Sagade, S.K. Samdarshi, P.S. Panja, Enabling rating of intermediate temperature solar cookers using different working fluids as test loads and its validation through a design change, Sol. Energy 171 (2018) 354–365, https://doi.org/10.1016/j.solener.2018.06.088.
[19] A.A. Sagade, S.K. Samdarshi, P.J. Lahkar, Ensuring the completion of solar cooking process under unexpected reduction in solar irradiance, Sol. Energy 179 (2019) 286–297, https://doi.org/10.1016/j.solener.2018.12.0.69.
[20] E. Vengadesan, R. Senthil, Experimental investigation of the thermal performance of a box type solar cooker using a finned cooking vessel, Renew. Energy 171 (2021) 431–446, https://doi.org/10.1016/j.renene.2021.02.130.
[21] H. Kurt, K. Atik, M. Özkaymak, Z. Recebli, Thermal performance parameters estimation of hot box type solar cooker by using artificial neural network, Int. J. Therm. Sci. 47 (2008) 192–200, https://doi.org/10.1016/j.ijthermalsci.2007.02.007.
[22] G. Coccia, G. Di Nicola, M. Pierantozzi, S. Tomassetti, A. Aquilanti, Design, manufacturing, and test of a high concentration ratio solar box cooker with multiple reflectors, Sol. Energy 155 (2017) 781–792, https://doi.org/10.1016/j.solener.2017.07.020.
[23] S. Kumar, Thermal performance study of box type solar cooker from heating characteristic curves, Energy Convers. Manag. 45 (2004) 127–139, https://doi.org/10.1016/S0196-8904(03)00103-1.
[24] M. Collares-Pereira, A.C., A. Tavares, Figures of merit and their relevance in the context of a standard testing and performance comparison methods for solar box – Cookers, Sol. Energy 166 (2018) 21–27, https://doi.org/10.1016/j.solener.2018.03.040.
[25] M.S. Al-Soud, E. Abdallah, A. Akayleh, S. Abdallah, E.S. Hrayshat, A parabolic solar cooker with automatic two axes sun tracking system, Appl. Energy 87 (2010) 463–470, https://doi.org/10.1016/j.apenergy.2009.08.035.
[26] G. Kumaresan, V.S. Vigneswaran, S. Esakkimuthu, R. Velraj, Performance assessment of a solar domestic cooking unit integrated with thermal energy storage system, J. Energy Storage 6 (2016) 70–79, https://doi.org/10.1016/j.est.2016.03.002.
[27] A. Saxena, E. Cuce, G.N. Tiwari, A. Kumar, Design and thermal performance investigation of a box cooker with flexible solar collector tubes: an experimental research, Energy 206 (2020) 118144, https://doi.org/10.1016/j.energy.2020.118144.
[28] A.G. Bhave, C.K. Kale, Development of a thermal storage type solar cooker for high temperature cooking using solar salt, Sol. Energy Mater. Sol. Cells 208 (2020) 110394, https://doi.org/10.1016/j.solmat.2020.110394.
[29] R Core Team, R: A Language and Environment for Statistical Computing, R Foundation for Statistical Computing, 2019 https://www.R-project.org/.
[30] J.A. Duffie, W.A. Beckman, Solar Engineering of Thermal Processes, fourth ed., Willey, 2013.
[31] Stockton Solar Oven Solar cooking Wiki https://solarcooking.fandom.com/wiki/Stockton_Solar_Oven s12 May 2021 Accessed
[32] GoSun Fusion Solar cooking Wiki https://solarcooking.fandom.com/wiki/GoSun_Fusion s13 May 2021 Accessed
[33] W.S. Cleveland, E. Grosse, W.M. Shyu, Local regression models, in: J.M. Chambers, T.J. Hastie (Eds.), Chapter 8 of Statistical Models in S, Wadsworth & Brooks/Cole, 1992.
[34] W.N. Venables, B.D. Ripley, Modern Applied Statistics with S, Springer, New York, 2002.